2004

Large Dielectric Constant and Maxwell-Wagner Relaxation in Bi2/3Cu3Ti4O12

Jianjun Liu
University of Nebraska-Lincoln, jliu@unlserv.unl.edu

Chun-Gang Duan
University of Nebraska at Omaha

Wei-Guo Yin
University of Nebraska at Omaha

Wai-Ning Mei
University of Nebraska at Omaha, physmei@unomaha.edu

Robert W. Smith
University of Nebraska at Omaha, robertsmith@unomaha.edu

See next page for additional authors

Large dielectric constant and Maxwell-Wagner relaxation in $Bi_{2/3}Cu_3Ti_4O_{12}$

Jianjun Liu,[1,2] Chun-Gang Duan,[1] Wei-Guo Yin,[1] W. N. Mei,[1] R. W. Smith,[3] and J. R. Hardy[2]
[1]*Department of Physics, University of Nebraska, Omaha, Nebraska 68182-0266, USA*
[2]*Department of Physics and Center for Electro-Optics, University of Nebraska, Lincoln, Nebraska 68588-0111, USA*
[3]*Department of Chemistry, University of Nebraska, Omaha, Nebraska 68182-0109, USA*
(Received 5 November 2003; revised manuscript received 9 June 2004; published 12 October 2004)

We studied frequency and temperature dependences of impedance, electric modulus, and dielectric permittivity of $Bi_{2/3}Cu_3Ti_4O_{12}$ in the ranges of $10^{-1}-10^6$ Hz and $-150-200\,^\circ$C, respectively. We first observed two electrical responses in the impedance and modulus formalisms. Then we detected a Debye-like relaxation in the permittivity formalism. Most interestingly, we found that the large dielectric constant of $Bi_{2/3}Cu_3Ti_4O_{12}$ is independent of the temperature and frequency below $150\,^\circ$C. The results are interpreted in terms of a two-layer model with conducting grains partitioned from each other by poorly conducting grain boundaries. Using this model, we attributed the two electrical responses in impedance and modulus formalisms to the grain and grain-boundary effects, respectively, while the detected Debye-like relaxation and large dielectric constant were well explained in terms of Maxwell-Wagner relaxation.

DOI: 10.1103/PhysRevB.70.144106 PACS number(s): 77.22.Ch, 72.80.Sk

I. INTRODUCTION

Since $CaCu_3Ti_4O_{12}$ (CCTO) was found to have a giant dielectric constant,[1,2] it has attracted much attention, not only because of the numerous potential technological applications of the materials with such properties, but also because of the origin of the giant dielectric constant. CCTO has a body-centered cubic perovskite-related structure. It shows an extremely high value (up to 10^5) for the permittivity ε' at room temperature in the frequency range between dc and 10^6 Hz. Furthermore, it was found that the permittivity is practically independent of temperature between 100 and 600 K. Usually large dielectric constants in perovskite materials are related to the atomic displacements within a noncentrosymmetrical structure, but the cubic structure of CCTO is stable down to 35 K. Thus this gives rise to a question: what is the mechanism of the giant dielectric constant?

Since structural[1] and spectroscopic investigations[3–5] have ruled out any anomalies in crystal structure and lattice vibrations, most explanations involve extrinsic mechanisms, e.g., Subramanian *et al.* suggested that the high dielectric constant could be due to creation of barrier layer capacitances, presumably at twin boundaries;[1] impedance measurement showed that CCTO ceramic was a single-step internal barrier layer capacitor where insulating grain boundaries partition the semiconducting grains;[6] Lunkenheimer *et al.* suggested that the colossal dielectric constant might be due to a Maxwell-Wagner-type contribution of depletion layers at the interface between sample and contacts or at grain boundaries;[7] Cohen *et al.* proposed that the giant dielectric constant might arise from spatial inhomogeneity of local dielectric response.[8] In addition, the extrinsic explanation was further supported by a recent experimental measurement[9] that the intrinsic dielectric constant of a perfect CCTO single-crystal film is only about 100, which is much smaller than the giant value observed in polycrystalline samples. However, none of the above mentioned proposals is widely accepted, and the nature of the extrinsic mechanism remains unsettled.

Recently, other materials with giant dielectric constants were also reported, for example, Li or Ti Doped NiO,[10] $AFe_{1/2}B_{1/2}O_3$ (A=Ba,Sr,Ca; B=Na,Ta,Sb),[11] $LaMnO_3$,[7] and $SrNbO_{3.41}$.[7] The interesting feature is that all these giant dielectric constant materials have similar dielectric behavior to CCTO, i.e., they all exhibit a Debye-like relaxation and their dielectric constants are nearly independent of frequency and temperature well below the relaxation frequency.

We also noticed that similar dielectric behavior was reported as early as in 1973 for yttrium iron garnet.[12] It was found to have a Debye-like relaxation, and its low-frequency dielectric constant was as high as 4000, and independent of temperature and frequency in the range of 274–363 K and $10^{-2}-10^2$ Hz. Larsen *et al.* interpreted the experimental results successfully by using Maxwell-Wagner relaxation,[13,14] which generally refers to interfacial polarization occurring in electrically inhomogeneous systems. When an electric current passes through interfaces between two different dielectric media, because of their different conductivities, surface charges pile up at the interfaces, and give rise to a Debye-like relaxation process under an external alternating voltage. This effect could be conveniently described by an equivalent circuit and has been widely used to account for dielectric relaxations in many heterogeneous materials.[7,11,15]

Subramanian *et al.* summarized 62 compounds with the CCTO structure in the $ACu_3M_4O_{12}$ system.[16] They found more than ten compounds have dielectric constants larger than 1000 at room temperature. However, they did not study the temperature and frequency dependence of the dielectric behavior. Their investigations pose the following questions: Why do the compounds in this system tend to have much larger dielectric constants than one expects based on the dielectric polarizabilities of their constituent atoms? Do they have similar temperature and frequency dependences in their dielectric behavior as CCTO? Do all the large dielectric constants result from a common mechanism? Since there are tremendous technical demands for large dielectric constant materials, it is interesting to investigate systematically the dielectric properties of compounds in the $ACu_3M_4O_{12}$ sys-

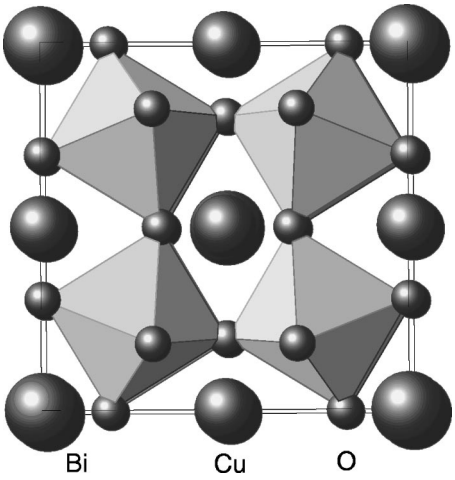

FIG. 1. Crystal structure of BCTO, in which 1/3 Bi sites are vacant. The Ti atoms sit at the center of the TiO_6 octahedra.

tem, which certainly will shed light on the origin of giant dielectric constant in CCTO.

We have studied the impedance, electric modulus, and permittivity of several compounds in the $ACu_3M_4O_{12}$ system. Preliminary results show that all the samples investigated display similar dielectric properties, namely, large dielectric constants independent of frequency and temperature in a wide range, but they differ in detail in their impedance and electric modulus spectra. In this work we report results on the compound $Bi_{2/3}Cu_3Ti_4O_{12}$ (BCTO) due to the fact that it can be clearly interpreted by the Maxwell-Wagner model. The results of other compounds require detailed analysis and will be reported later.

BCTO crystallizes as cubic perovskite-related structure as shown in Fig. 1 with space group *Im*3 and lattice constant $a=7.413$ Å. [1,16] In this structure, the Bi sites are 1/3 vacant in order to achieve charge neutrality. This might affect the dielectric behavior, rendering the study of this sample more interesting. The dielectric constant of BCTO was reported to be 1871 at 25 °C and 10^5 Hz.[1] Although it is not as high as that of CCTO, it is still much larger than ordinary dielectrics.

In Sec. II of this article, we briefly describe the experimental method. In Sec. III, we first report the experimental results on the impedance and electric modulus spectra which reveal the existence of electrical inhomogeneity in BCTO ceramic sample, then, we explain the dielectric permittivity spectra in terms of the Maxwell-Wagner model. Finally, we present the conclusion in Sec. IV.

II. EXPERIMENT

Polycrystalline samples of BCTO were prepared by solid-state reaction. The starting materials Bi_2O_3, CuO, and TiO_2 were dried before being weighed and mixed thoroughly in an agate mortar. The mixture was calcined in air at 950–1000 °C for 20 h with intermediate grinding. The final sample was ground into powder, checked by x-ray diffraction, and pressed into disks of 10 mm diameter/0.5 mm thickness. The disks were sintered at 1100 °C for 10 h.

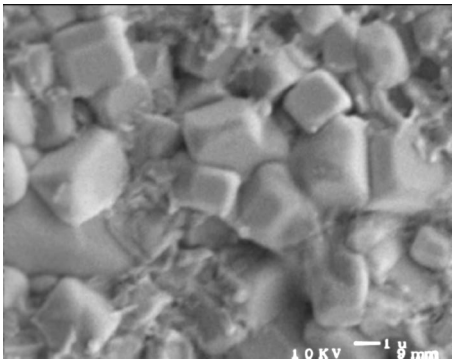

FIG. 2. SEM image of microstructure for BCTO pellet.

Scanning electron microscopy (SEM) (Model: JEOL JSM840A) performed at 10 kV was used to determine the grain size in an as-prepared pellet. Surfaces of the pellet were gold coated prior to the SEM examination. The microstructure of BCTO pellet is presented in Fig. 2, which shows that grain sizes are in the range of 2–4 μm.

Complex impedance was measured using a NOVOCONTROL alpha high resolution dielectric analyzer (Alpha-S) in the temperature range −150–200 °C and the frequency range 10^{-1}–10^6 Hz. Silver paint was used on the polished surfaces as electrodes.

The complex impedance Z^* of the sample was obtained in the usual way, i.e., $Z^*=V^*/I^*$, where V^* and I^* are the applied voltage and the resulting current, respectively. Then the complex electric modulus M^* and complex permittivity ε^* were calculated as follows:

$$M^* = M' + iM'' = i\omega C_0 Z^*, \tag{1}$$

$$\varepsilon^* = \varepsilon' - i\varepsilon'' = \frac{1}{i\omega C_0 Z^*}, \tag{2}$$

where ω is the angular frequency $\omega=2\pi f$ and $i=\sqrt{-1}$. $C_0=\varepsilon_0 S/d$ is the empty cell capacitance, where S is the sample area and d the sample thickness.

III. RESULTS AND DISCUSSION

A. Impedance formalism

In Fig. 3 we present the frequency dependence of the imaginary part (Z'') of the impedance $Z^*=Z'-iZ''$ at different temperatures. We observe at −150 °C a weak peak at about 10^5 Hz, shifting to higher frequencies with decreased intensity as the temperature increases. At −70 °C it moves out of the frequency range of our experiment. When the temperature is increased above 0 °C, another strong peak appears in the measured frequency range as shown in Fig. 3(b), which also moves to higher frequencies with a fall in intensity as the temperature increases. This implies both electrical responses are thermal activated.

The complex impedance plane plots (Z'' vs Z') are given in Fig. 4. Usually a conduction process results in a semicircular arc in a linear complex plane plot. The log-log presentation in Fig. 4 enables us to compare two responses with

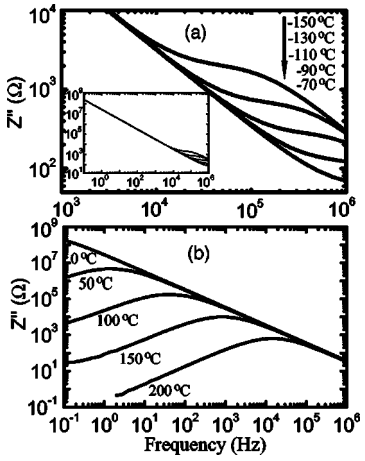

FIG. 3. Frequency dependence of imaginary part (Z'') of impedance Z^* at different temperatures.

vastly different impedances in one plot. Although the semicircular arcs are distorted, logarithmic plot still offers significant advantages in several respects which have been discussed by Jonscher.[17] In Fig. 4, we observe that below −100 °C the plots consist of segments of a small arc and a big arc. This can be seen more clearly in the insert, which is a linear Z'' vs Z' plot at −150 °C. The ratio of the diameters of the two arcs exceeds 10^5 at −150 °C, which indicates that the resistance associated with the big arc is much larger than that of the small arc. Both arcs shift from right to left with reduced diameters as the temperature increases due to the associated decreases of the impedances. Similar phenomena were observed in CCTO.[6]

To analyze the impedance spectra, data usually are modeled by an ideal equivalent circuit consisting of a resistor R and a capacitor C. Because polycrystalline materials generally show intergranular or grain-boundary impedances, they can be represented by the equivalent circuit shown in Fig. 5.[18,19] The circuit consists of a series array of two subcircuits, one represents grain effects and the other represents grain boundaries. Each subcircuit is composed of a resistor and capacitor joined in parallel. Let (R_g, R_{gb}) and (C_g, C_{gb}) be the resistances and capacitances of grains and grain boundaries, respectively, then the impedance Z^* for the equivalent circuit in Fig. 5 is[18]

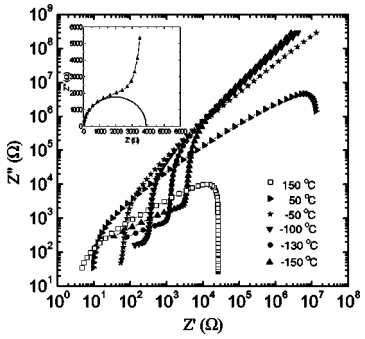

FIG. 4. Log-log complex impedance plane plot (Z'' vs Z') at different temperatures.

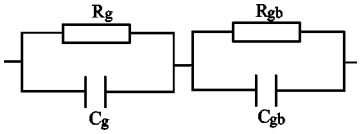

FIG. 5. Equivalent circuit used to represent the electrical properties of grain and grain-boundary effects.

$$Z^* = \frac{1}{R_g^{-1} + i\omega C_g} + \frac{1}{R_{gb}^{-1} + i\omega C_{gb}} = Z' - iZ'', \tag{3}$$

where

$$Z' = \frac{R_g}{1 + (\omega R_g C_g)^2} + \frac{R_{gb}}{1 + (\omega R_{gb} C_{gb})^2} \tag{4}$$

and

$$Z'' = R_g\left[\frac{\omega R_g C_g}{1 + (\omega R_g C_g)^2}\right] + R_{gb}\left[\frac{\omega R_{gb} C_{gb}}{1 + (\omega R_{gb} C_{gb})^2}\right]. \tag{5}$$

Based on Eq. (5), the response peaks of the grains and grain boundaries are located at $1/(2\pi R_g C_g)$ and $1/(2\pi R_{gb} C_{gb})$, respectively, and the peak values are proportional to associated resistances. In general, the peak frequency for grain boundaries is much lower than that for grains due to their large resistance and capacitance compared with those of grains.[6] Therefore, in the impedance spectra, we attribute the higher frequency response, which corresponds to the small arc in Fig. 4, to the grains, and the lower one to the grain boundaries. Comparing the peak values of the two responses, we estimate that below 0 °C the resistance of grain boundaries is at least 10^5 times larger than that of grains, i.e., $R_{gb} \gg R_g$.

As shown in Fig. 3, response peaks from the grains are too weak to be analyzed by using Eq. (5). Above 0 °C, the strong peaks from grain boundaries move into the measured frequency range, while the grain peaks have already moved out. Hence we can fit the Z'' to a single $R_{gb}C_{gb}$ parallel circuit. For an ideal $R_{gb}C_{gb}$ parallel circuit, the electrical response is of the Debye-type,

$$Z^* = \frac{R_{gb}}{1 + i\omega R_{gb} C_{gb}}. \tag{6}$$

However, we found that Z'' is better described by using the Cole-Cole equation,[20] which is commonly used for polycrystalline samples,[19]

$$Z^* = \frac{R_{gb}}{1 + (i\omega\tau_{gb}^z)^\alpha}, \tag{7}$$

where $\tau_{gb}^z = R_{gb}C_{gb}$ and the parameters α, $0 < \alpha \leqslant 1$, is used to measure the departure from the ideal Debye response. This implies that the response from the grain boundaries is not of the ideal Debye type. In other words, the grain boundaries cannot be described by ideal RC elements. The fitted values of α at different temperatures are in the range of 0.80–0.86 and increase with increasing temperature.

By fitting the experimental data to Eq. (7), we obtained the resistance R_{gb} and the response time $\tau_{gb}^z = R_{gb}C_{gb}$ at different temperature. R_{gb} decreases from 1.3×10^8 Ω at 20 °C

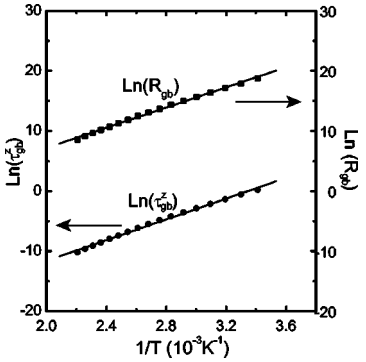

FIG. 6. Arrhenius plot of resistance R_{gb} and relaxation time τ^z_{gb} of grain boundaries from impedance spectra.

to $5.4\times10^3\ \Omega$ at 180 °C, meanwhile, τ^z_{gb} reduces from 1.2 s to 3.8×10^{-5} s. We found both R_{gb} and τ^z_{gb} follow the Arrhenius law

$$\tau = \tau_0 e^{(E/k_B T)}, \tag{8}$$

where τ_0 is the prefactor, E denotes the activation energy for the response, k_B is Boltzman constant, and T is absolute temperature. In Fig. 6 we plot the ln τ^z_{gb} and ln R_{gb} vs $1/T$, in which the solid lines are the fitted results using Eq. (8). From the slopes of the fitted straight lines we obtain an activation energy of 0.73 eV for τ^z_{gb} and that of 0.72 eV for R_{gb}. Two nearly equal activation energies reveal that the resistance and response time decrease at a similar rate, which implies the capacitance C_{gb} has a rather weak temperature dependence. Compared to our results, the activation energy of CCTO grain boundaries was reported to be 0.60 eV.[6]

B. Electric modulus formalism

As shown in Sec. III A, the peak intensities in Z'' arising from the grains are very weak due to the small resistance of grains relative to that of grain boundaries. However, we shall see in the following that the grain effects will be magnified in the electric modulus formalism ($M^*=M'+iM''$), rendering them easier to be analyzed. The M^* representation was originally introduced by Macedo *et al.* to study space-charge relaxation phenomena.[21] It is now often used together with the impedance and permittivity formalisms to separate grain and grain-boundary effects and/or to distinguish the microscopic processes responsible for localized dielectric relaxations and long-range conductions.[22] We have applied this technique to the investigations of $Bi_2Ti_4O_{11}$, and observed several interesting features in relaxation and conducting processes.[23]

Based on Eqs. (1) and (3) the electric modulus $M^*=M'+iM''$ of the equivalent circuit in Fig. 5 is[18]

$$M' = \frac{C_0}{C_g}\left[\frac{(\omega R_g C_g)^2}{1+(\omega R_g C_g)^2}\right] + \frac{C_0}{C_{gb}}\left[\frac{(\omega R_{gb} C_{gb})^2}{1+(\omega R_{gb} C_{gb})^2}\right] \tag{9}$$

and

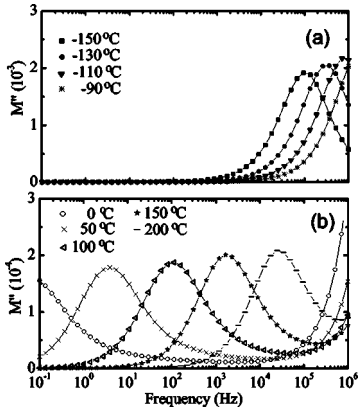

FIG. 7. Frequency dependence of imaginary part (M'') of electric modulus M^* at different temperatures.

$$M'' = \frac{C_0}{C_g}\left[\frac{\omega R_g C_g}{1+(\omega R_g C_g)^2}\right] + \frac{C_0}{C_{gb}}\left[\frac{\omega R_{gb} C_{gb}}{1+(\omega R_{gb} C_{gb})^2}\right]. \tag{10}$$

From Eq. (10), we can easily see that the response peaks of the grains and grain boundaries in M'' also occur at frequencies $1/(2\pi R_g C_g)$ and $1/(2\pi R_{gb} C_{gb})$, respectively. Since peak values are proportional to the reciprocals of the associated capacitances, the smaller capacitance should dominate in the electric modulus plots. The grains usually have smaller capacitance than the grain boundaries, thus their response peaks show up stronger in the modulus spectra.

In Fig. 7, we show the frequency dependence of M'' at different temperatures. As in the impedance formalism, the response frequencies of grains and grain boundaries almost fall into two different frequency ranges. Strong grain peaks occur below −90 °C [Fig. 7(a)], whereas, those from grain boundaries emerge above 0 °C [Fig. 7(b)]. All the peaks shift to higher frequencies with increasing temperature. In addition, the peak values of M'' depend only slightly on temperature, which implies that capacitances of grains and grain boundaries only weakly depend on temperature. Furthermore, the intensities of the grain peaks are nearly ten times greater than those from grain boundaries. This indicates that the grain capacitance is roughly ten times smaller than that of the grain boundaries. Since the grains and grain boundaries are not really ideal RC elements, as we found in the impedance spectra, we observe that the shapes of the M'' peaks are broader than Debye peak. This broadening of the response might be due to an inherently nonexponential process, such as correlation between diffusive motion of the ions, or nonuniformities in the material microstructure, leading in turn to a spatial distribution of local conductivities and electrical response times.[24]

In Fig. 8 we show the complex plane plot M'' vs M' at −150, 10, and 50 °C. We observed a big semicircle at −150 °C which originates from the grain effect. At this temperature, the response of grain boundaries is still out of the measured frequency range. When the temperature is increased to 50 °C, the grain peaks has moved out of, while the grain-boundary peak has completely entered the mea-

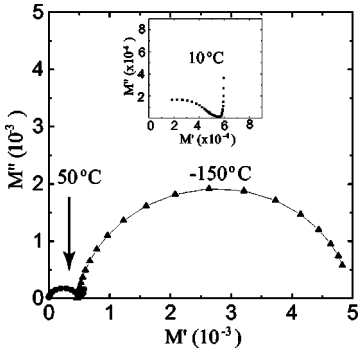

FIG. 8. Complex electric modulus plane plot (M'' vs M') at -150, 10, and 50 °C.

sured frequency range and forms a small semicircle as indicated by the arrow in Fig. 8. The different capacitances of grains and grain boundaries give rise to arcs of different diameters in the plot. Between −150 °C and 50 °C, the plots consist of segments of the big and small arcs such as the one shown in the insert in Fig. 8.

In the M'' vs f plot, the electrical response peak reaches its maximum when the condition $2\pi f_{max}\tau=1$ is fulfilled. Based on this condition, we derived the most probable conductivity relaxation times τ_g^m and τ_{gb}^m for grains and grain boundaries, respectively, from the peak frequencies f_{max}. Figure 9 presents their dependences on reciprocal temperature, and shows that τ_g^m and τ_{gb}^m also closely follow the Arrhenius law [Eq. (8)]. From the slopes of fitted straight lines, we obtain the activation energy for grains is 0.092 eV and that for grain boundaries is 0.73 eV, which is consistent with the value 0.73 eV obtained in the impedance formalism. The grain activation energy 0.092 eV of our sample is close to 0.08 eV of CCTO grains.[6]

C. Permittivity formalism

After studying the impedance Z^* and modulus M^* of our sample, we proceed to the complex permittivity $\varepsilon^*=\varepsilon'-i\varepsilon''$, which was obtained from the impedance spectra by using Eq. (2).

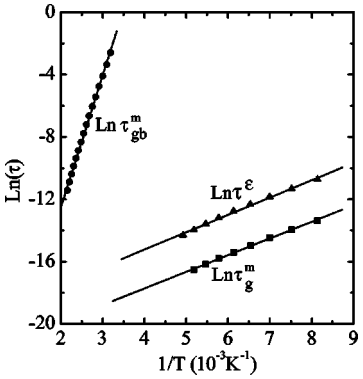

FIG. 9. Arrhenius plot of relaxation times τ_g^m and τ_{gb}^m from electric modulus spectra and dielectric relaxation time τ^{ε} from permittivity spectra.

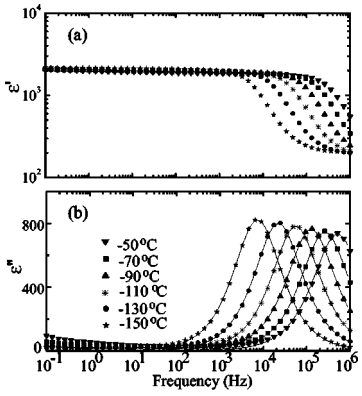

FIG. 10. Frequency dependence of permittivity ε^* at different temperatures. (a) Real part ε', (b) imaginary part ε''.

In Fig. 10, we presented the frequency dependence of ε' and ε'' of BCTO at different temperatures. ε'' clearly shows a Debye-like relaxation peak shifting to higher frequencies with increasing temperature. Correspondingly, ε' decreases from a constant value at low frequency to a small saturated value at high frequency.

The temperature dependences of the dielectric permittivity ε' and ε'' for different frequencies are shown in Fig. 11. ε' shows a step increase from about 100 to about 1790 at fixed frequency as shown in Fig. 11(a). Meanwhile, ε'' shows a peak which shifts to high temperature with increasing frequency. At room temperature and 10^5 Hz, ε' is about 1750 close to the reported value of 1871.[16] We found that the saturated values of ε' hardly depend on the temperature and frequency below 150 °C. All these dielectric behaviors are similar to those found in the giant dielectric constant materials reported before, such as yttrium iron garnet,[12] CCTO,[1,2] Li or Ti Doped NiO,[10] and $A\mathrm{Fe}_{1/2}B_{1/2}\mathrm{O}_3$ (A=Ba, Sr, Ca; B=Na, Ta, Sb).[11]

The frequency dependence of the observed dielectric relaxation shown in Fig. 10(b) can be represented by the empirical Cole-Cole relation,[20]

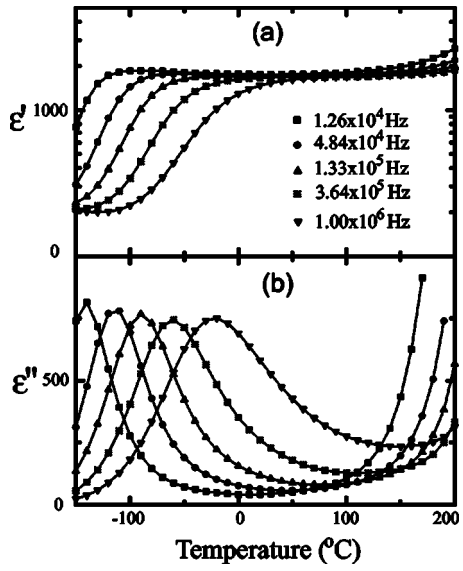

FIG. 11. Temperature dependence of permittivity ε^* at different frequencies. (a) Real part ε', (b) imaginary part ε''.

$$\varepsilon^*(\omega) = \varepsilon'(\omega) - i\varepsilon''(\omega) = \varepsilon_\infty + \frac{\varepsilon_s - \varepsilon_\infty}{1 + (i\omega\tau^{\varepsilon})^{\gamma}}, \tag{11}$$

where ε_s and ε_∞ are the static- and high-frequency limits of the dielectric constant, respectively, τ^{ε} is the most probable relaxation time, γ is a constant with values between 0 and 1. For an ideal Debye relaxation $\gamma=1$. $\gamma<1$ implies that the relaxation has a distribution of relaxation time, leading to a broader peak shape than Debye peak. The solid curves in Fig. 10(b) are the fitted results for ε''. The fitted γ values are in the range of 0.85–0.9 at different temperatures. The fitted τ^{ε} also follows the Arrhenius law in Eq. (8) as shown in Fig. 9 and the activation energy is 0.095 eV, which is close to that of grains (0.092 eV) obtained from the modulus spectra.

In Secs. III A and III B we have shown that BCTO is electrically inhomogeneous. It consists of conducting grains and poorly conducting grain boundaries, which can be described by the equivalent circuit in Fig. 5. Therefore, we continue to use this equivalent circuit to interpret the dielectric results.

We can calculate the permittivity ε^* of the equivalent circuit in Fig. 5 by using Eqs. (2) and (3), which can be presented in the following form:[25]

$$\varepsilon^*(\omega) = \varepsilon'_\infty + \frac{\varepsilon'_s - \varepsilon'_\infty}{1 + i\omega\tau} - i\frac{\sigma'}{\omega}, \tag{12}$$

where

$$\varepsilon'_\infty = \frac{1}{C_0}\frac{1}{\dfrac{1}{C_g} + \dfrac{1}{C_{gb}}}, \tag{13}$$

$$\varepsilon'_s = \frac{R_g^2 C_g + R_{gb}^2 C_{gb}}{C_0 (R_g + R_{gb})^2}, \tag{14}$$

$$\sigma' = \frac{1}{C_0 (R_g + R_{gb})}, \tag{15}$$

$$\tau = \frac{R_g R_{gb}(C_g + C_{gb})}{R_g + R_{gb}}, \tag{16}$$

where ε'_s,ε'_∞ are the static- and high-frequency permittivity, respectively, σ' is ohmic conductivity, and τ the time constant.

Equation (12) shows that the equivalent circuit in Fig. 5 gives a relaxation spectrum similar to the Debye relaxation even without any dipole relaxation. This process is called Maxwell-Wagner relaxation as we discussed in Sec. I, which often occurs in the heterogeneous systems in which the component dielectrics have different conductivities.[25,26] Therefore, one can assert that a detected Debye-like relaxation response is not necessarily the result of dipole relaxation in the system, sometimes, it can be attributed to the heterogeneity of the system, for example, grain boundaries and/or the electrodes applied to the sample. We attribute the observed peaks in Fig. 10 to Maxwell-Wagner relaxation because the sample consists of conducting grains and poorly conducting grain boundaries. The observed relaxation peaks represented by Eq. (11) are broader than those given by Eq. (12) since the grains and grain boundaries cannot be represented by ideal RC elements as discussed in Sec. III A. We shall show below that the relaxation time τ [Eq. (16)] of the Maxwell-Wagner relaxation is approximately determined by the product of the resistance of the grains R_g and the capacitance of the grain boundaries C_{gb}. Therefore, distributions of grain size and conductivity or even inhomogeneous conductivity of the grains may cause a distribution of relaxation times τ and lead to broader relaxation peaks.[15]

From Secs. III A and III B we learn that $R_{gb} \gg R_g$, and $C_{gb} \approx 10 C_g$. Therefore, the effective dielectric permittivity of the sample at frequencies much lower than the relaxation frequency $1/(2\pi\tau)$ can be approximated from Eq. (14),

$$\varepsilon'_s \approx \frac{C_{gb}}{C_0}, \tag{17}$$

thus ε'_s is determined only by the ratio between the grain-boundary capacitances C_{gb} and the vacuum capacitance of the sample C_0. Hence ε'_s is constant when C_{gb} is temperature and frequency independent. This result is excellently consistent with our experiment, namely, we observed a constant dielectric constant in wide temperature and frequency ranges due to the nearly unchanged C_{gb}.

Moreover, if we assume that grains and grain boundaries form a two-layer capacitor with thickness $(d_g + d_{gb})$, where d_g and d_{gb} are the thickness of the grains and the grain-boundary layers, respectively, from Eq. (17), $\varepsilon'_s \approx \varepsilon_{gb}(d_g + d_{gb})/d_{gb}$, its ε_{gb} is the dielectric constant of the grain-boundary layer. Therefore, even a small dielectric constant ε_{gb} can lead to a giant effective dielectric constant ε'_s if the ratio $(d_g + d_{gb})/d_{gb}$ is large. For example, if the grain is about 10 μm, the boundary region is about 100 Å, and $\varepsilon_{gb}=10$, then $\varepsilon'_s \approx 10000$. This might explain the giant dielectric constant of CCTO ceramics. Similar suggestion was made by Raevski *et al.*[11] In our sample, the ratio $(d_g + d_{gb})/d_{gb}$ might not be as large as that in CCTO, so the dielectric constant is much smaller.

Also, by using the conditions $R_{gb} \gg R_g$ and $C_{gb} \approx 10 C_g$, we can approximately obtain the time constant τ from Eq. (16),

$$\tau \approx R_g C_{gb}. \tag{18}$$

Since the conduction relaxation times of the grains $\tau_g^m = R_g C_g$ follows the Arrhenius law, while C_g is weakly temperature dependent, we deduce that R_g follows the Arrhenius law, Eq. (8). Let $R_g = R_g^0 \exp(E_g/k_B T)$ (R_g^0 is prefactor and E_g the activation energy of the grain conduction process), then we obtain from Eq. (18)

$$\tau \approx R_g C_{gb} \approx C_{gb} R_g^0 e^{(E_g/k_B T)}. \tag{19}$$

Equation (19) shows that the activation energy of the dielectric process approximately equals that of the grain conduction process. This result is in good agreement with our results that the grain conduction activation energy of (0.092 eV) is close to that of the dielectric process (0.095 eV).

IV. CONCLUSION

We have investigated the temperature and frequency dependences of the impedance, electric modulus, and permittivity spectra of polycrystalline $Bi_{2/3}Cu_3Ti_4O_{12}$. We found that the sample is electrically inhomogeneous because two conduction processes in the impedance and modulus spectra were detected. We attributed them to grain and grain-boundary effects, respectively, and deduced their activation energies from the Arrhenius law. We also observed that there is a Debye-like relaxation in the permittivity spectra, and that the dielectric constant is independent of frequency and temperature below the relaxation frequency. We explained these experimental results by using Maxwell-Wagner model and suggested that same model governs the giant dielectric constant in CCTO.[1,2]

ACKNOWLEDGMENTS

This work was supported by the Nebraska Research Initiative, the Nebraska-EPSCoR-NSF Grant No. EPS-9720643 and the U.S. Army Office under Grant Nos. DAAG 55-98-1-0273, DAAG 55-99-1-0106, and DAAD 19-02-1-0099. We thank Dr. X. Z. Li for his help on SEM experiment in Center for Materials Research and Analysis, University of Nebraska-Lincoln.

[1] M. A. Subramanian, Dong Li, N. Duan, B. A. Reisner, and A. W. Sleight, J. Solid State Chem. **151**, 323 (2000).
[2] C. C. Homes, T. Vogt, S. M. Shapiro, S. Wakimoto, and A. P. Ramirez, Science **293**, 673 (2001).
[3] A. P. Ramirez, M. A. Subramanian, M. Gardel, G. Blumberg, D. Li, T. Vogt, and S. M. Shapiro, Solid State Commun. **115**, 217 (2000).
[4] N. Kolev, R. P. Bontchev, A. J. Jacobson, V. N. Popov, V. G. Hadjiev, A. P. Litvinchuk, and M. N. Iliev, Phys. Rev. B **66**, 132102 (2002).
[5] C. C. Homes, T. Vogt, S. M. Shapiro, S. Wakimoto, M. A. Subramanian, and A. P. Ramirez, Phys. Rev. B **67**, 092106 (2003).
[6] D. C. Sinclair, T. B. Adams, F. D. Morrison, and A. R. West, Appl. Phys. Lett. **80**, 2153 (2002).
[7] P. Lunkenheimer, V. Bobnar, A. V. Pronin, A. I. Ritus, A. A. Volkov, and A. Loidl, Phys. Rev. B **66**, 052105 (2002).
[8] Morrel H. Cohen, J. B. Neaton, Lixin He, and David Vanderbilt, J. Appl. Phys. **94**, 3299 (2003).
[9] A. Tselev, C. M. Brooks, H. Zheng, L. Salamanca-Riba, S. M. Anlage, and R. Ramesh, cond-mat/0308057.
[10] Junbo Wu, Ce-Wen Nan, Yuanhua Lin, and Yuan Deng, Phys. Rev. Lett. **89**, 217601 (2002).
[11] I. P. Raevski, S. A. Prosandeev, A. S. Bogatin, M. A. Malitakaya, and L. Jastrabik, J. Appl. Phys. **93**, 4130 (2003).
[12] P. K. Larsen and R. Metselaar, Phys. Rev. B **8**, 2016 (1973).
[13] J. C. Maxwell, *Electricity and Magnetism* (Oxford University Press, Oxford, England, 1873), Vol. I, sec. 328.
[14] K. W. Wagner, Ann. Phys. (Leipzig) **40**, 53 (1913).
[15] H. Neumann and G. Arlt, Ferroelectrics **69**, 179 (1986).
[16] M. A. Subramanian and A. W. Sleight, Solid State Sci. **4**, 347 (2002).
[17] A. K. Jonscher, *Dielectric Relaxation in Solids* (Chelsea Dielectric Press, London, 1983), p. 83.
[18] D. C. Sinclair and A. R. West, J. Appl. Phys. **66**, 3850 (1989).
[19] J. Ross Macdonald, *Impedance Spectroscopy* (Wiley, New York, 1987).
[20] K. S. Cole and R. H. Cole, J. Chem. Phys. **9**, 341 (1941).
[21] P. B. Macedo, C. T. Moynihan, and R. Bose, Phys. Chem. Glasses **13**, 171 (1972).
[22] R. Gerhardt, J. Phys. Chem. Solids **55**, 1491 (1994).
[23] Jianjun Liu, Chun-gang Duan, Wei-guo Yin, W. N. Mei, R. W. Smith, and J. R. Hardy, J. Chem. Phys. **119**, 2812 (2003).
[24] C. T. Moynihan, Solid State Ionics **105**, 175 (1998).
[25] Von Hippel, *Dielectrics and Waves* (Wiley, New York, 1954).
[26] E. Billig and K. W. Plessner, Proc. Phys. Soc. London **64B**, 361 (1951).